# Multi-Multigrid Solution of Modified Poisson–Boltzmann Equation for Arbitrarily Shaped Molecules

**SEBASTIAN TOMAC, ASTRID GRÄSLUND**

*Department of Biophysics, Stockholm University, S-10691 Stockholm, Sweden*

*Received 21 August 1997; accepted 16 January 1998*

**ABSTRACT:** A new multi-multigrid method is presented for solving the modified Poisson–Boltzmann equation based on the Kirkwood Hierarchy of equations, with Loeb's closure, on a three-dimensional grid. The results are compared with standard Poisson–Boltzmann calculations, which are known to underestimate the local concentration of counterions near charged parts of molecules, mainly due to neglect of fluctuations in the ionic concentrations. In the present study, the Kirkwood hierarchy of equations is discretized with the finite volume method and solved using multigrid techniques. The new possibility for solution of the three-dimensional modified Poisson–Boltzmann equation, for the first time within a model including a dielectric discontinuity, and within reasonable computational time, enables the calculation of higher valence ion distributions around arbitrarily shaped biological macromolecules. © 1998 John Wiley & Sons, Inc. J Comput Chem 19: 893–901, 1998

**Keywords:** Poisson–Boltzmann; electrostatics; Kirkwood; Loeb; multigrid; multivalent ions

## Introduction

Electrostatics is of great importance for macromolecular interactions and energetics.[1,2] The nonlinear Poisson–Boltzmann equation has been used widely and successfully for studying ionic effects on stability and energetics of biological macromolecules. However, standard Poisson–Boltzmann calculations are known to underestimate the local concentration of counterions near charged parts of molecules, mainly due to neglect of fluctuations in the ionic concentrations.[2] Extending the applicability of the Poisson–Boltzmann equation beyond monovalent ion solutions of low to medium concentration is desirable considering the biological importance of higher va-

*Correspondence to*: A. Gräslund

Contract/grant sponsor: Swedish Natural Science Research Council

Contract/grant sponsor: Carl Trygger Foundation



CCC 0192-8651 / 98 / 080893-09

lence ions. Such extension is possible by introducing corrections for the ion fluctuation. Modified Poisson–Boltzmann equations based on the Kirkwood hierarchy,[3] together with linearized Loeb's closure (weak ion–ion coupling),[4] have been developed and used for describing the distribution of ions around systems of spherical, cylindrical, and planar geometry, giving good correlation with Monte Carlo and hypernetted chain simulations for higher valence ions.[5–7] The advance of fast computers and the development of efficient finite-difference algorithms[8–13] for solving the nonlinear as well as the linearized Poisson–Boltzmann equation have opened the possibility for the solution of the full Kirkwood hierarchy of equations on a three-dimensional grid.

In this study we introduce a multi-multigrid solution of the Kirkwood hierarchy of equations with Loeb's closure for arbitrary geometry. The equations are discretized with a finite-difference algorithm and the numerical solutions of the equations are accomplished by multigrid techniques. Under conditions of a homogeneous dielectric medium the computational outcome is compared and found to agree closely with earlier modified Poisson–Boltzmann studies on systems with spherical symmetry, as well as grand canonical monte carlo simulations on a primitive salt solution containing divalent ions. The present study provides, for the first time, an algorithm that makes it possible to calculate the distribution of higher valence ions around a macromolecule of arbitrary shape.

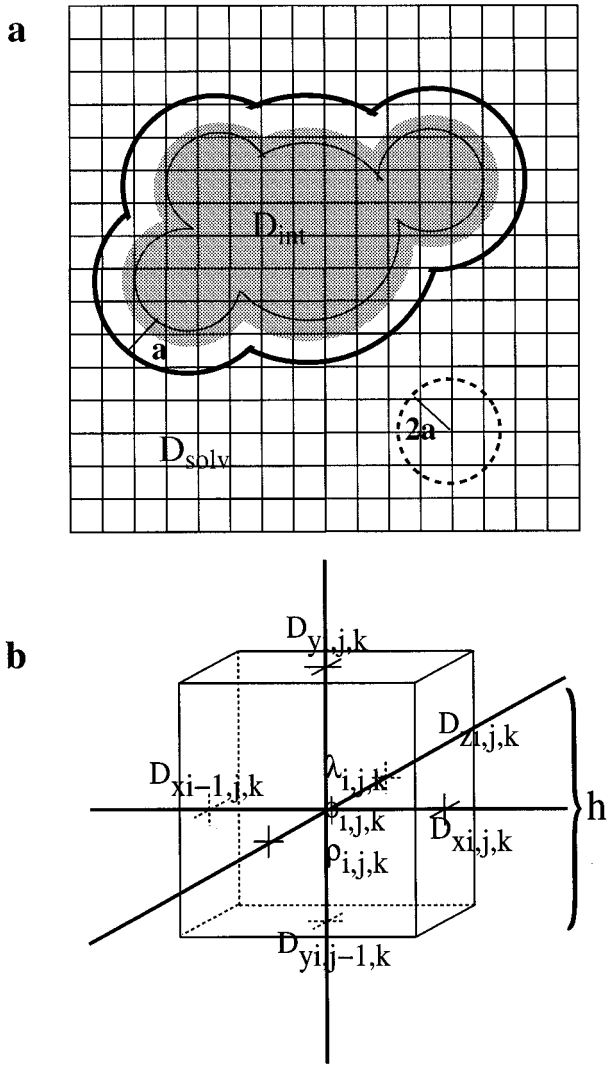


**FIGURE 1.** (a) Grid slice through a Debye–Hückel model of the macromolecule. Gray areas denote internal dielectric constant (i.e., inside a 1-Å water layer and the van der Waals radius of the fixed atoms). Grid lines crossing the dielectric interface by a fraction of the grid spacing are given an intermediate dielectric constant. Mobile ions access grid points outside a shell of thickness of the mobile ions (a). The dotted line circle of radius **2a** illustrates an example of a temporary fixed mobile ion centered on a grid node. (b) Grid element of size $h$, each grid point $(i, j, k)$ is given a potential $(\phi)$, fixed charge $(\rho)$, and a logic parameter $(\lambda)$ containing boolean values for whether the point is accessible or inaccessible to mobile ions, whether or not the point is a dielectric border point, and whether the point is inside a temporary fixed mobile ion. If the point is situated next to a dielectric interface, three dielectric constants $(D_x, D_y, D_z)$ are assigned with a logic parameter flagging whether the particular line crosses the dielectric interface.

## Theory

### POISSON EQUATION

Consider a system of charged colloidal particles, defined by the fixed coordinates of their boundaries. The particles form a dielectric cavity of dielectric constant $D_{\text{int}}$, embedded in a strong electrolyte solution consisting of $n$ species of ion **i** in a solvent of temperature $T$ and dielectric $D_{\text{solv}}$, as illustrated in Figure 1a. The Poisson equation establishes a relationship between the mean electrostatic potential at a point **r** in the solvent and the singlet distribution $g_i(r)$ of the ions with respect to the reference or bulk concentration $C_i^o$ of the hypothetical reservoir as follows:

$$-\nabla \cdot D(r)\nabla\psi(r) = \frac{\rho^f(r)e}{kT\varepsilon_o} \qquad (1a)$$

(valid inside the van der Waals radius of the macromolecule and a shell of thickness **a**). And:

$$-\nabla \cdot D(r)\nabla\psi(r) = \sum_i \frac{e}{kT\varepsilon_o} eZ_i n_i^o g_i(r) \quad (1b)$$

(valid outside the macromolecule and with a shell of thickness **a**). Eq. (1a) applies inside the boundary of the fixed ions and a shell of thickness **a**, where **a** is the mobile ion radius, and eq. (1b) applies in the solution accessible for the mobile ions, as illustrated in Figure 1. $D(r)$ is the dielectric constant, $\psi(r)$ is the mean electrostatic potential in e/kT units; $\rho^{(f)}(r)$ is the fixed ion density; $e$ is the elementary charge; $k$ is Boltzmann's constant; $T$ is the absolute temperature; $Z$ is the ionic charge; and $n_i^o = C_i^o N_A 1000$, where $N_A$ is Avogadro's number; and $C_i^o$ is the molar concentration. All entries are expressed in SI units. Fixed charges are treated explicitly, whereas the mobile charges are only treated implicitly, as a continuum solvent. The electrostatic free energy can be obtained either by integrating over the fixed charges or by volume integration.[14,15] If the single ion distribution is restricted to the form $g_i(r) = g_i(r)[\psi(r), r]$ we may define[14]:

$$\Delta\Pi(\psi, r) = \sum_i n_i^o \int_v dr \int^{\psi} d\psi g_i[\psi(r), r] \quad (2)$$

The electrostatic free energy can be expressed as:

$$\Delta G = \int_\nu dr\rho^f(r)\psi(r) - \frac{\varepsilon_o}{2}\int_\nu dr\psi(r)\nabla \cdot D(r)\nabla\psi(r) - \Delta\Pi_i(\psi, r) \quad (3)$$

where $\Delta$ denotes the subtraction of a reference state electrostatic free energy, in this case the absence of mobile ions.

In this study, we use a finite volume discretization approach, and a multigrid techniques are employed for numerical solution of discrete equations.

## METHOD FOR SOLVING THE POISSON EQUATION

Multigrid methods are highly efficient computational techniques for solving nonlinear elliptic differential equations. Multigrid methods have previously been used for solving the Poisson–Boltzmann equation, both the linearized form[8] and the nonlinear form.[9,10] A general description of the multigrid technique may be found in *Numerical Recipes in C*.[16]

For clarity, we will be explicit with the protocol used in solving the relevant equations. Eqs. (1a) and (1b) may be symbolically written as:

$$L(u) = f \quad (4)$$

where $L(u)$ is composed of the potential dependent terms;

$$L(u) = -\Delta D(r) \cdot \nabla\psi(r) - \sum_i \frac{e}{kT\varepsilon_o} eZ_i n_i^o g_i(r) \quad (5)$$

and $f$ is the source term, $\rho^f$ in eq. (1a). The continuous equations are discretized on a grid of mesh size $h$, for example, $L(\hat{u}_h) = f_h$, where $\hat{u}_h$ denotes the exact solution of the potential on the discrete grid.

Figure 2 illustrates multigrid cycle protocols. For the solution of the Poisson equation in the

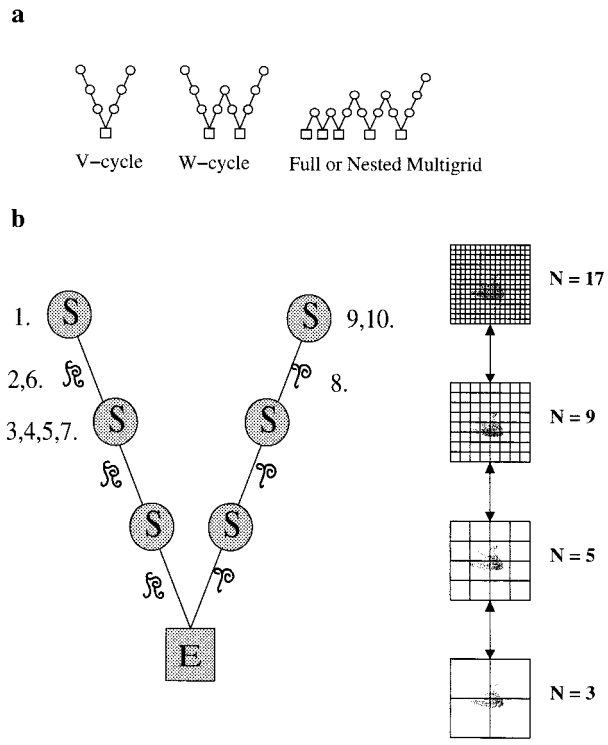


**FIGURE 2.** (a) Structure of multigrid cycles. The finest grid is at the top level of each diagram. The nested multigrid cycles were used for solving the Poisson equation in the absence of salt. Poisson–Boltzmann as well as Loeb's closure equations were solved using a *V*-cycle grid. (b) Detailed *V*-cycle for a grid with the finest grid size of $17^3$. S denotes smoothing, *E* denotes the exact solution on the finest grid, $\Re$ denotes restriction, and $\wp$ denotes prolongation. Numbers 1–10 are detailed in the text.

absence of mobile ions a nested multigrid is used, and in the presence of mobile ions a full approximation storage *V*-cycle scheme is performed, as illustrated in Figure 2b. For the finitized eq. (1) on a grid of mesh $h$, given a proximate solution of the discrete equation, a residual is generated as:

$$L(u_h) = r_h \tag{6}$$

where the source term is included in the residual. Finitized eq. (1) on grid point $o$ maybe written as:

$$r_h + \frac{e^2 q_0^f}{\varepsilon_o kTh^3} = \frac{\sum_{j=1}^{6} D_j \psi_0}{h^2} - \frac{\sum_{j=1}^{6} D_j \psi_j}{h^2} \tag{7}$$

(inside the fixed ions and with a shell of thickness **a**). And:

$$r_h = \frac{\sum_{j=1}^{6} D_j \psi_0}{h^2} - \frac{\sum_{j=1}^{6} D_j \psi_j}{h^2} - \sum_i \frac{e}{\varepsilon_o kT} e Z_i n_i^0 g_i(r) \tag{8}$$

(outside the fixed ions and with a shell of thickness **a**), where $D_j$ is the dielectric constant assigned to the line between grid point $o$ and the neighbor $j$ summing over all six neighboring points, as illustrated in Figure 1b. In the special case of a grid point where all neighboring grid lines have the same dielectric constant $D$, the sum $\sum D\psi$ reduces to $6D\sum\psi$ and, hence, the number of multiplications per iteration is reduced to $1/6$. Such a protocol of stripping[13] is implemented in the case of different dielectric constants assigned to the volume inside and outside the cavity formed by the fixed charges. For each grid point a logic bit value is assigned for being inside or outside the fixed reference ions and the shell of radius **a**, and also a boolean value for being inside or outside the dielectric cavity. Three bits are used to flag whether the lines to neighboring points, denoted $x$, $y$, $z$ in Figure 1b, cross the dielectric boundary. Grid lines crossing the dielectric interface are given an intermediate value, as described previously.[11] The matrix containing the logic information is restricted to the coarser grids using straight injection. The logic values flagging whether the points are on a dielectric boundary, are remapped on each grid level. The strong discontinuity in the dielectric coefficients caused the multigrid methods to exhibit poor convergence.[17] Using a harmonic averaging operator upon the restriction of the grid line dielectric coefficients improves convergence properties, as discussed previously.[8]

Figure 2b illustrates the *V*-cycle full-approximation multigrid scheme used. The values in the protocol in what follows correspond to those given for a two-grid cycle in Figure 2b. For some initial guess of $u_h^o$ on the finest grid, the following cycles are repeated until convergence:

1. Presmooth. As smoothing operator, a one-step newtonian Gauss–Seidel operator is used:

$$u_h^{new} = u_h - \frac{L(u_h)}{\partial L(u_h)/\partial u_h}$$

2. The newly calculated $L(u_h)$ and $u_h$, as well as the residual $r_h$, are restricted by the half-weight restriction operator ($\Re$).
3. The relative residual caused by the coarsening of the grid is estimated by:

$$\tau_h = \Re[\,L(u_h)] - L(\Re u_h)$$

4. The residual $r_H$ of the coarse grid ($H$) is formed by adding the relative truncation error $\tau_h$ to the restricted residual:

$$r_H = \Re r_h + \tau_h$$

5. The equation is solved analytically if on the coarsest grid ($3^3$).
6. The error induced by the interpolation from the coarser to the finer grid is estimated by restricting the fine-grid $\Re u_h$.
7. On the coarse grid a restriction–prolongation correction term may be calculated as:

$$v_h = u_H - \Re u_h$$

8. Prolongation of the correction term $\wp v_h$. It is common to let the prolongation operator $\wp$ be the adjoint of the restriction operator.
9. The fine grid potentials are upgraded:

$$u_k^{new} = u_h - \wp v_h$$

10. Postsmoothing.

In the full-approximation storage multigrid algorithm both the residual and the relaxed approximation $u_h$ have to be restricted to the coarser grid. Hence, in the solving of $u_H$ we solve for the full approximation and not just the error introduced by the coarsening. This point is crucial for an efficient algorithm solving the Kirkwood hierarchy

of equations discussed next. Convergence is accepted when the relative residual of the $j$th iteration falls below 1.0E-7, and is defined as:

$$\left\| \frac{r_h^j}{f_h} \right\| = \frac{\| f_h - L_h u_h^j \|}{\| f_h \|} \tag{9}$$

The grid sizes are multiples of $(n - 1)$ with coarsest grid size of $3^3$. Normally, the equations are solved on a $65^3$ grid.

## KIRKWOOD HIERARCHY OF EQUATIONS

From the Kirkwood charging process,[3] an expression for the singlet ion distribution is:

$$g_i(r) = \zeta_i^o(r) \exp(-Z_i \psi(r) - \Delta\varphi_i(r)) \tag{10}$$

where $Z_i$ is the ion valence, $\psi(r)$ the mean electrostatic potential, and $\Delta\varphi_i$ the ''fluctuation term,'' both in $e/kT$ units. $\zeta_i^o(r) = g_i(r \mid Z_i e = 0)$ is an exclusion volume term given as[3]:

$$\zeta_i^o(r) = 1 - 2 \sum_i \frac{2\pi}{3} n_i^o (2a)^3 (g_i(r) - 1) \tag{11}$$

if the ions are treated as rigid spheres. The resulting equation from including eq. (10) in the Poisson equation will henceforth be referred to as the Kirkwood equation. If the terms $\zeta$ and $\Delta\varphi$ are ignored we have an expression equivalent to the nonlinear Poisson–Boltzmann equation (NLPB):

$$g_i(r) = \exp(-Z_i \psi(r)) \tag{12}$$

The fluctuation term, $\Delta\varphi$,[3, 6] is given by the charging integral over the fluctuation potential, $\phi_i(r_1, r_2)$ (in e/kT units), at $r_2$, given a mobile ion held temporary fixed at $r_1$, as:

$$\Delta\varphi_i(r_2) = \int_0^{Z_i} \lim_{r_1 \to r_2} (\phi_i^*(r_1, r_2) - \phi_{bulk}^*(r_1, r_2)) \tag{13}$$

where $\phi_i^*(r_1, r_2) = \phi_i(r_1, r_2) - eZ_i/D\varepsilon_o|r_1 - r_2|$; for example, the subtraction of the Coulomb self-potential. The reference in this case is when the mean potential is set to zero with bulk concentration of the mobile ions. An expression for the fluctuation potential is obtained using nonlinear Loeb's closure (NLLC) as follows[4]:

$$-\nabla \cdot D(r_2) \nabla \phi_\alpha(r_1, r_2) = 0 \tag{14a}$$

(valid inside the fixed ions and with a shell of thickness **a**). And:

$$-\nabla \cdot D(r_2) \nabla \phi_i(r_1, r_2) = \frac{e^2}{kT\varepsilon_o} Z_i(r_2) - \nabla \cdot D(r_2) \nabla \psi(r) \tag{14b}$$

(valid outside the fixed ions and with a shell of thickness **a**, but inside the temporary fixed mobile ion and its shell of thickness 2**a**). And:

$$-\nabla \cdot D(r_2) \nabla \phi_\alpha(r_1, r_2) = \sum_i \frac{e}{kT\varepsilon_o} e Z_i n_i^o g_i(r) (\exp(-Z_i \phi_\alpha(r_1, r_2)) - 1) \tag{14c}$$

(valid outside all fixed ions, temporary and permanent, and with a shell of thickness **a**, as illustrated in Fig. 1a). A reasonable approximation of eq. (14c) is the linearized version of Loeb's closure (LLC):

$$-\nabla \cdot D(r_2) \nabla \phi_i(r_1, r_2) = -\phi_i(r_1, r_2) \kappa^2 \tag{14d}$$

where $\kappa^2$ is the modified Debye–Hückel parameter:

$$\kappa^2 = \sum_i \frac{e^2 Z_i^2}{kT\varepsilon_o} n_i^o g_i(r) \tag{15}$$

It is possible to obtain the fluctuation term by numerically performing charging integration over the given fixed mobile charge,[18] using fluctuation potentials obtained from the numerical solution of the LLC equation for a given temporarily fixed ion. It is, however, computationally more convenient to use the variational method,[14, 15] which requires only one solution of the LLC equation for a given fixed mobile ion to calculate the fluctuation term. We use volume integration in our calculations. In complete analogy with eq. (3) the ''fluctuation term'' is given by:

$$\varphi = \int_\nu dr Q(r_2) \phi(r_1, r_2) - \frac{\varepsilon_o}{2} \int_\nu dr \phi(r_1, r_2) \nabla \cdot D(r_2) \nabla \phi(r_1, r_2) - \Pi(\phi, r_1, r_2) \tag{16}$$

where $Q(r)$ corresponds to the right-hand side of eq. (14b). Assuming the single ion distribution, $g_i(r)$, to be dependent only on the fluctuation potential, $\phi_i(r_1, r_2)$, for the linearized Loeb's clo-

sure the fluctuation term is given by:

$$\varphi = \frac{1}{2}\int_{\nu} drQ(r_2)\phi(r_1, r_2) \qquad (17)$$

The $\Delta\varphi$ is obtained by subtracting the reference state fluctuation obtained with a mean potential of zero. For the solution of the Kirkwood hierarchy the LLC equation has to be solved, holding a mobile ion temporary fixed, for every point in solution. Within the finite-difference treatment of Poisson's equation employed here the mobile ion of species **i** is temporarily held fixed and centered on every grid node situated outside the macromolecule and the shell of thickness **a** surrounding it.

This calculation creates an enormous computational burden, and a number of numerical approximations are introduced to reduce the number of grid nodes upon which the equation has to be solved, as discussed in the next subsection.

## METHODS FOR SOLVING THE KIRKWOOD HIERARCHY OF EQUATIONS

A multi-multigrid scheme is developed as follows. A grid spacing of less than 1.1 Å is used. Initially, the nonlinear Poisson–Boltzmann equation is solved using a *V*-full multigrid.[8] This gives the initial (henceforth referred to as the 0th iteration) estimates of the mean potential on the finest grid. Subsequently, the Kirkwood equation is solved as the last post-Newtonian Gauss–Seidel smoothing sweep in a *V*-cycle on the finest grid. Thus, for every grid point the fluctuation term is calculated by solving the LLC equation for an ion of species *i*, centered on the grid node, surrounded by a 2**a**-thick mobile ion-exclusion layer as illustrated in Figure 1a. This is done for every ion species, and in all cases the bulk reference fluctuation term is subtracted. After solution of the LLC equation for the given ion, the $\Delta\varphi$ is updated on the major grid. The calculated $\Delta\varphi$ values are restricted to the coarser grids by a half-weighting restriction operator and treated as constants during the Kirkwood equation multigrid *V*-cycles, whereby the mean potential $\psi(r)$ is solved for the given fluctuation term. This procedure, including updating of the fluctuation terms in the last *V*-cycle smoothing, is repeated until the relative residual is less than 1.0E-4, on the finest grid.

To reduce the number of grid points on which the LLC equation must be solved and reduce the computational time for solving the LLC equation, the following approximations are made. The LLC equation is solved on an $(N + 1)/2$ grid (where $N$ is the major grid size), centered on the temporary fixed mobile ion, with a box side length corresponding to that of the major grid. Grid points lying at a distance of less than 2**a** to the edge of the box are given a fluctuation term with a value of zero. Grid points closer to the macro-ion surface than a distance of 2**a** are solved on a grid size of $N$. Grid points with a $|\nabla D(r)\ \nabla\psi(r)|$, above some threshold value are also given a fluctuation term of zero value. The threshold is chosen such that the proximate resulting fluctuation term would change the single ion distribution at $< 0.01$. In case of a major grid of $65^3$ the fluctuation term is calculated on the $33^3$ grid using the mean potential on the 33 grid as the source term. The calculated fluctuation terms are interpolated to the finer $65^3$ grid. For distances of less than 2**a** from the macromolecule the fluctuation terms are recalculated on a $33^3$ side grid. In should be stressed that such a protocol requires the use of the full approximation storage multigrid, because the source term for the given coarser grid must correspond to the current solution of the mean electrostatic potential on that grid. Approximately three to sour *V*-cycles are required for convergence. This procedure was implemented in the MIST program.

## TEST PROBLEMS

The calculations were performed on an SGI 02 computer (180 MHz MIPS R5000). The algorithm was written in C/C++. On such a machine the solution for a sphere in homogeneous dielectric on a $65^3$ grid took approximately 64 CPU s for the linearized Poisson–Boltzmann or LLC equation and approximately 154 CPU s for the NLPB, measured using the C-clock subroutine. With multigrid the CPU time per grid point was independent of grid size.[8] For the Kirkwood hierarchy of equations, the LLC equation had to be solved on a side grid for every major grid point, in every *V*-cycle step. Taken together the solution of the Kirkwood hierarchy of equation on a $33^3$ major grid, with side grids having a size of $17^3$, took approximately 4 hours for a sphere in homogeneous dielectric. We used the convention of writing major grid (the grid on which the macromolecule is mapped) first, followed by the side grid (the grid upon which the temporary fixed ion is centered); for example, 33(17) for a major grid of $33^3$ and a side grid of $17^3$, except at a distance of less than 2**a** where a

side grid size of $33^3$ was used. Test calculations were performed on a sphere with a radius of 5 Å and charge of 4.143e, corresponding to a surface charge density of 0.22 $C/m^2$ in homogeneous dielectric of 78.5, at a temperature of 298 K, for comparability with an earlier study.[6] The sphere was centered on the major grid in a solution of mobile ions of varying valence and concentration with a radius of 2.125 Å. For comparisons with primitive salt grand canonical Monte Carlo simulations, calculations were performed on a 2.1 Å, −1e-sphere in a homogeneous dielectric of 78.65 and temperature of 298.15 K. The procedure used in the Monte Carlo simulations followed the protocol given in an earlier publication by Valleau and Cohen.[19]

As an illustration of solving the equation for arbitrary geometry and the effects of discontinuous dielectric (i.e., formation of a dielectric cavity by the fixed ions) calculations were made on an adenosine triphosphate molecule (ATP).[20] The ATP with a well-defined three-dimensional structure formed a dielectric cavity with a dielectric constant of 2 inside the van der Waals radius and a water shell of 1.0 Å,[21,22] surrounded by a solvent dielectric of 78, in a solution of 2:1 salt (e.g., $MgCl_2$) of 0.05*M*, with a mobile ion radius of 2.1 Å and temperature of 298.15 K. The charges assigned to the molecule were taken from the AMBER force field.[23] The net charge of the ATP molecule was −3e.

The box boundary points were either given a potential of zero or, if mentioned, were approximated in the case of a uniform dielectric by the analytical solution of the Debye–Hückel equation:

$$\psi(R) = \sum_{i=1}^{N_q} \frac{\exp(-\kappa|R - r_i|)}{D_{out}|R - r_i|} \qquad (18)$$

where $\kappa$ is the Debye length, $R$ the border point, and $r_i$ the ion coordinate, summing over all $N$ ions. In case of solving the LLC equation the temporary fixed mobile ion grid border points were always given a fluctuation potential of zero.

## Results and Discussion

Verification of the algorithm was accomplished by comparing the calculated single ion distribution function of a sphere using the three-dimensional Kirkwood hierarchy solver with the previously calculated values, as seen in Figure 3. Figure 3a shows the mean electrostatic potential, from the three-dimensional Kirkwood solution on grids of varying size for a sphere in 1*M* 1:1 salt. Figure 3b shows the resulting single-ion radial distribution function. The results were compared with earlier published spherical modified Poisson–Boltzmann results,[6] as well as with only solving the NLPB equation. Good correlation was found between grids of size 33(17) and 65(17), except in the close

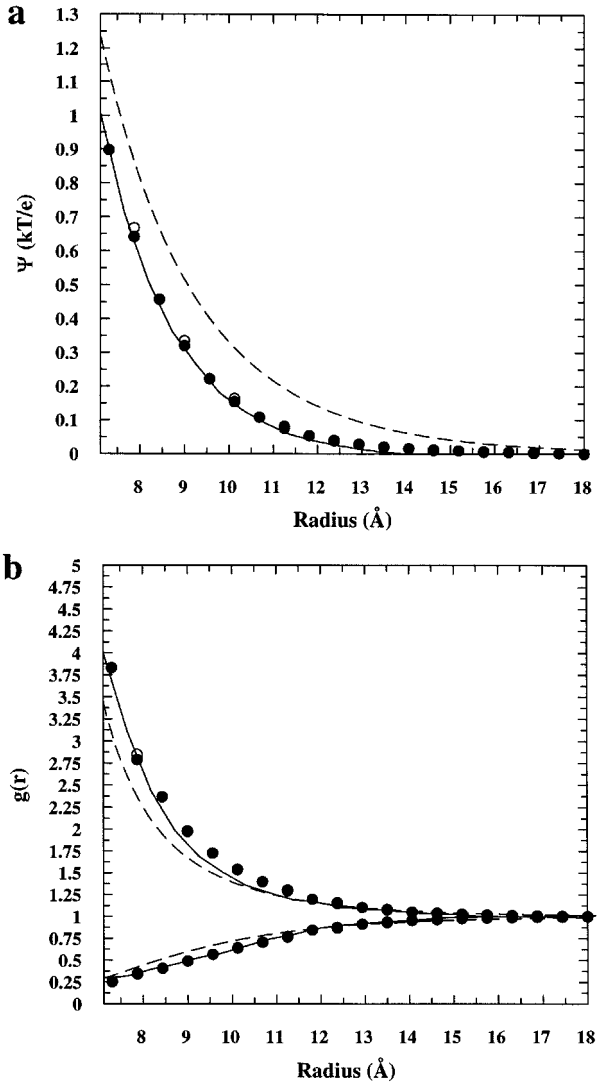


**FIGURE 3.** (a) Mean electrostatic potential and (b) single-ion distribution functions from the NLPB (---), the Kirkwood hierarchy on a 33(17) grid (•) and on a 65(17) grid (o), and the modified Poisson–Boltzmann equation (——) [from C. W. Outhwaite and L. B. Bhuiyan, *Mol. Phys.*, **74**, 367 (1991)], in a solution of a 1:1 electrolyte at a concentration of $C_o$ = 1.0*M* and a mobile ion radius of **a** = 2.125 Å, with a central sphere of charge 4.314e and a radius of 5 Å.

vicinity of the macromolecule. Smaller grids consistently overestimated the fluctuation term.

Figure 4 shows a comparison between the Kirkwood hierarchy results and a grand canonical Monte Carlo simulation, for the radial distribution of a 2:1 salt around a sphere with a 2.1 Å radius, and charge −1e. The Monte Carlo protocol used, and the dimensions of the primitive salt solution investigated corresponded to those from an earlier study.[19] The Kirkwood equation results correlated well with those obtained from the Monte Carlo simulation, except in the vicinity of the macro-ion where it overestimated the concentrations, to some extent caused by the finite grid size. As pointed out earlier, the Poisson–Boltzmann method underestimates the concentration of counterions close to the macro-ion. It should be noted that the Monte Carlo calculations could only be performed assuming a homogeneous dielectric constant and, consequently, this condition was also used in the multigrid calculations. A more detailed comparative study with Monte Carlo results will be published elsewhere. The good agreement between the three-dimensional Kirkwood hierarchy results and the earlier results from modified Poisson–Boltzmann as well as Monte Carlo calculations for simpler systems like the spherical macro-ion, and continuous dielectric constant, shows that the new method gives satisfactory performance.

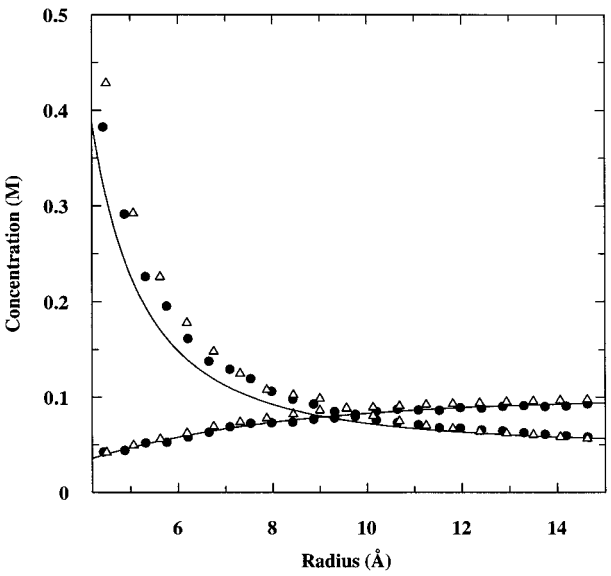


**FIGURE 4.** NLPB (——) on a 65 grid, a Kirkwood hierarchy on 65(17) grid (Δ), and grand canonical Monte Carlo (•) radial concentration of mobile ions, in a solution of 2:1 electrolyte at a concentration of $C_o = 0.05M$ and a mobile ion radius of **a** = 2.1 Å, with a central sphere of charge −1.0e and a radius of 2.1 Å.

For testing the numerical accuracy of using coarser grids for calculating the fluctuation potentials, fluctuation terms were calculated using different grid sizes, as shown in Figure 5. In all cases, we consider the 0th iteration (i.e., when the mean potential was given from the solution of the NLPB equation). The calculations were performed on a major grid of size $65^3$, with varying sizes of the minor grid. Side grids of sizes 17, 33, and 65 were compared. There was a systematic overestimation of the fluctuation term on the smaller grids as compared with the largest. The error increased with proximity fo the macro-ion. By using a finer side grid in the vicinity of the macro-ion, a maximum deviation was observed of approximately 1% to the finest grid in the resulting single-ion radial distribution, using the protocol described in the previous section. For testing the use of volume integration for calculating the fluctuation term [eq. (17)] the value was compared with the results from the charging integral [eq. (13)] for a temporary le mobile ion on a point situated 9 Å from the center of the fixed reference sphere. The charging integral method gave values identical to those obtained with volume integration.

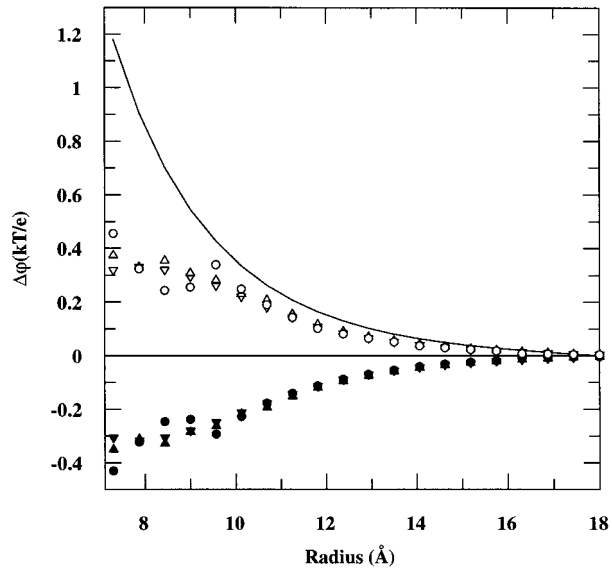


**FIGURE 5.** The 0th iteration fluctuation terms, where mean electrostatic potential is given from NLPB (——) on a $65^3$ grid. Fluctuation term distribution function for co-ions (unfilled symbols) and counterions (filled symbols), calculated on 65(17) (o), 65(33) (Δ), and 65(65) (∇) grids, in a solution of 1:1 electrolyte at a concentration of $C_o = 1.0M$ and a mobile ion radius of **a** = 2.125 Å, with a central sphere of charge 4.314e and a radius of 5 Å.

The improved aspects of the new method (i.e., the treatment of arbitrarily shaped molecules in a dielectric discontinuous medium were demonstrated by solving the Kirkwood hierarchy of equations, which were solved for an ATP molecule on a $65^3$ grid, forming dielectric cavity of $D_{int} = 2.0$ in a solution of $D_{solv} = 78.0$ in a solution of $0.05M$ 2:1 salt. Figure 6 shows the single-ion distribution function, radially extending from the phosphates of the ATP molecule. These results were compared with those obtained from the NLPB equation. The local concentration of the divalent counterions near the negatively charged phosphates, obtained from the solution of the Kirkwood hierarchy of equations, was higher than the concentration obtained from solving of the NLPB equation. This should correspond to a more relistic description of the system.

The application and numerical realization of numerical solution of the Kirkwood hierarchy of equations indicates that the method is quite efficient for studying the interaction between macromolecules and multivalent ions. The possibility of solving the full Kirkwood hierarchy of equations, within a model including dielectric discontinuity and within reasonable computational time, suggests that it could be of great value for calculation of higher valence ion distributions around large biological macromolecules.

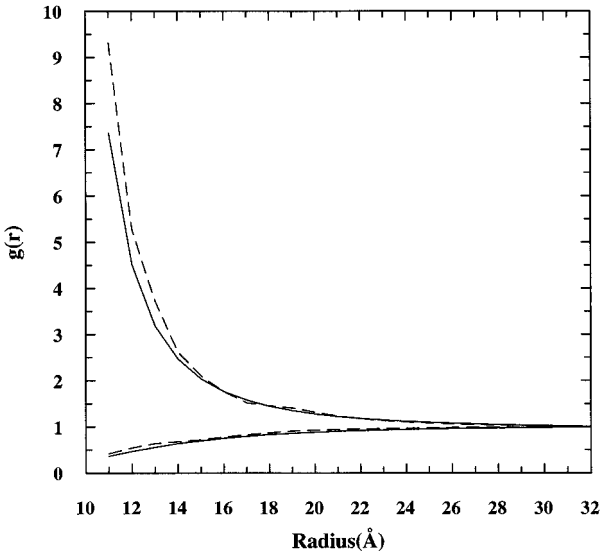


**FIGURE 6.** Radial single-ion distribution function for a line perpendicular to adenosine passing through the phosphate of an ATP molecule, from NLPB (——) on a $65^3$ grid, and Kirkwood hierarchy on a 65(17) grid (---) where the molecule forms a dielectric cavity of dielectric constant of 2 in the solvent of the dielectric constant of 78, in a solution of 2:1 electrolyte at a concentration of $C_o = 0.05M$ and a mobile ion radius of **a** = 2.1 Å.

## Acknowledgments

The authors are grateful to J. A. McCammon for providing us with a copy of the UHBD program. We also thank M. Holst for providing us with a copy of his mgZbase program.

## References

1. B. Honig and A. Nicholls, *Science*, **286**, 1144 (1995).
2. M. E. Davis and J. A. McCammon, *Chem. Rev.*, **90**, 509 (1990).
3. J. G. Kirkwood, *J. Chem. Phys.*, **2**, 767 (1934).
4. A. L. Loeb, *J. Coll. Sci.*, **6**, 75 (1951).
5. S. Levine and C. W. Outhwaite, *J. Chem. Soc. Faraday Trans.*, **74**, 1670 (1978).
6. C. W. Outhwaite and L. B. Bhuiyan, *Mol. Phys.*, **74**, 367 (1991).
7. T. Das, D. Bratko, L. B. Bhuiyan, and C. W. Outhwaite, *J. Phys. Chem.*, **99**, 410 (1995).
8. M. Holst and F. Saied, *J. Comput. Chem.*, **14**, 105 (1993).
9. H. Oberoi and N. M. Allewell, *Biophys. J.* **65**, 48 (1993).
10. M. Holst, R. E. Kozack, F. Saied, and S. Subramaniam, *Proteins*, **18**, 231 (1994).
11. M. E. Davis and J. A. McCammon, *J. Comput. Chem.* **10**, 386 (1989).
12. B. A. Luty, M. E. Davis, and J. A. McCammon, *J. Comput. Chem.*, **13**, 1114 (1992).
13. A. Nicholls and B. Honig, *J. Comput. Chem.*, **12**, 435 (1991).
14. E. S. Reiner and C. J. Radke, *J. Chem. Soc. Faraday Trans.*, **86**, 3901 (1990).
15. K. A. Sharp and B. Honig, *J. Phys. Chem.*, **94**, 7684 (1990).
16. W. H. Press, S. A. Teukolsky, W. T. Vetterling, and B. P. Flannery, *Numerical Recipes in C*, 2*nd Ed.*, Cambridge University Press, New York, 1992.
17. R. E. Alcouffe, A. Brandt, J. E. Dendy Jr., and J. W. Painter, *SIAM J. Sci. Statist. Comp.*, **2**, 430 (1981).
18. P. Debye and E. Hückel, *Phys. Z.*, **24**, 185 (1923).
19. J. P. Valleau and K. L. Cohen, *J. Chem. Phys.*, **72**, 5935 (1980).
20. J. Zheng, D. R. Knighton, L. F. Ten Eyck, R. Karlsson, N. Xuong, S. S. Taylor, and J. M. Sowadski, *Biochemistry*, **32**, 2154 (1993).
21. I. Klapper, R. Haagström, R. Fine, K. Sharp, and B. Honig, *Proteins*, **1**, 47 (1982).
22. B. Jayaram, K. A. Shap, and B. Honig, *Biopolymers*, **28**, 975 (1989).
23. S. J. Weiner, P. A. Kollman, D. A. Case, U. C. Singh, C. Ghio, G. Alagona, S. Profeta. Jr., and P. Weiner, *J. Am. Chem. Soc.*, **106**, 765 (1984).